

Yale University

EliScholar – A Digital Platform for Scholarly Publishing at Yale

Yale Medicine Thesis Digital Library

School of Medicine

2005

Association between human sperm morphology and aneuploidy using fluorescent In Situ hybridization

Jillian S. Catalanotti
Yale University

Follow this and additional works at: <http://elischolar.library.yale.edu/ymtdl>

Recommended Citation

Catalanotti, Jillian S., "Association between human sperm morphology and aneuploidy using fluorescent In Situ hybridization" (2005).
Yale Medicine Thesis Digital Library. 2447.
<http://elischolar.library.yale.edu/ymtdl/2447>

This Open Access Thesis is brought to you for free and open access by the School of Medicine at EliScholar – A Digital Platform for Scholarly Publishing at Yale. It has been accepted for inclusion in Yale Medicine Thesis Digital Library by an authorized administrator of EliScholar – A Digital Platform for Scholarly Publishing at Yale. For more information, please contact elischolar@yale.edu.

MED
T113
+Y12
7173

YALE UNIVERSITY LIBRARY



39002079490679

Association Between Human Sperm Morphology and
Azoospermia Using Fluorescent In Situ Hybridization

Jillian S. Catalanotti

YALE UNIVERSITY

2005

YALE
UNIVERSITY




CUSHING/WHITNEY
MEDICAL LIBRARY

Permission to photocopy or microfilm processing of this thesis for the purpose of individual scholarly consultation or reference is hereby granted by the author. This permission is not to be interpreted as affecting publication of this work or otherwise placing it in the public domain, and the author reserves all rights of ownership guaranteed under common law protection of unpublished manuscripts.

Julian Catalano
Signature of Author

03/08/05
Date



Digitized by the Internet Archive
in 2017 with funding from
The National Endowment for the Humanities and the Arcadia Fund

**Association Between Human Sperm
Morphology and Aneuploidy
Using Fluorescent *In Situ* Hybridization**

A Thesis Submitted to the
Yale University School of Medicine
In Partial Fulfillment of the Requirements for the
Degree of Doctor of Medicine

By
Jillian S. Catalanotti

2005

YALE MEDICAL LIBRARY

AUG 10 2005

T 113

+ Y12

7173

ABSTRACT

ASSOCIATION BETWEEN HUMAN SPERM MORPHOLOGY AND ANEUPLOIDY USING FLUORESCENT *IN SITU* HYBRIDIZATION. Jillian S. Catalanotti, Ciler Celik-Ozenci, and Gabor Huszar. Sperm Physiology Laboratory, Department of Obstetrics and Gynecology, Yale University, New Haven, CT.

With the increased use of assisted reproduction technology requiring manual sperm selection based on sperm shape, such as intracytoplasmic sperm injection (ICSI), a potential relationship between sperm morphology and chromosomal abnormalities is a major concern. In order to assess the feasibility of simultaneous evaluation of both attributes in an individual sperm cell, we investigated whether sperm shape is preserved after decondensation and denaturation as required for fluorescent *in situ* hybridization (FISH). We studied 395 spermatozoa using computer assisted morphometry, considering various head size, shape, and roundness parameters. Decondensation and denaturation were then performed, and sperm that were studied initially were re-localized and measured. To establish whether sperm of normal and abnormal shapes would behave in a similar manner in response to decondensation, the sperm were classified according to their head shapes into symmetrical (n=115), asymmetrical (n=115), irregular (n=115) and amorphous (n=50) categories. Initial shape was preserved in all morphological categories as measured either by shape factor (asymmetrical: 0% change, $p > 0.05$; irregular: 1.2% change, $p > 0.05$), by roundness ratio (symmetrical: 0% change, $p > 0.05$), or by both (amorphous: 0% change in roundness ratio, $p > 0.05$, 1.3% change in shape factor, $p > 0.05$). Overall, decondensation according to the FISH protocol does not significantly change sperm shape. FISH can be used to evaluate a potential relationship between sperm morphology and numerical chromosomal abnormalities in an individual sperm.

ACKNOWLEDGEMENTS

I would like to thank my parents, sisters, and grandparents for their emotional (and financial) support. Thanks to the YSM students who have made my time at Yale wonderful, especially Mandy Krauthamer, Michael Herce, Cinthia Guzman, Eric Golding, and Allyson Bloom; and to Chris Fonzone, who has made my time away from Yale even better.

I would also like to thank Dr. Gabor Huszar for his guidance as Principal Investigator of this study and as my thesis advisor. Thanks to Ciler Celik-Ozenci for her instruction, patience, and friendship throughout this work. This research would not be possible without the help of Lynne Vigue and Attila Jakab.

Funding for this work was primarily provided by National Institutes of Health Grants HD-19505, HD-32902, and OH-04061 (all to Dr. Gabor Huszar). This work was also supported by an NIH-NHLBI Medical Student Research Training Fellowship.

TABLE OF CONTENTS

Introduction	1
▪ <i>Intracytoplasmic Sperm Injection</i>	
▪ <i>Sperm Maturation</i>	
▪ <i>Sperm Morphology</i>	
▪ <i>Biochemical Markers of Sperm Maturity</i>	
▪ <i>HspA2 and Morphology</i>	
▪ <i>Role of HspA2 in Meiosis</i>	
▪ <i>Bridging Morphology and Numerical Chromosomal Abnormalities</i>	
▪ <i>Fluorescent In Situ Hybridization</i>	
Study Aims	10
Methods	11
▪ <i>Study Population</i>	
▪ <i>Preparation of Slides</i>	
▪ <i>Imaging of Sperm</i>	
▪ <i>Decondensation</i>	
▪ <i>Calibration</i>	
▪ <i>Computerized Morphometry Measurements</i>	
▪ <i>Morphological Classification by Sperm Head</i>	
▪ <i>Statistical Analysis</i>	
▪ <i>Denaturation</i>	
▪ <i>Validation of Methods</i>	
▪ <i>FISH Studies</i>	
Results	21
▪ <i>Decondensation and Relocalization of Sperm Fields</i>	
▪ <i>Controls</i>	
▪ <i>Decondensation Increases Sperm Size</i>	
▪ <i>Conservation of Sperm Shape after Decondensation</i>	
▪ <i>FISH Observations</i>	
Discussion	29
References	33

INTRODUCTION

Intracytoplasmic Sperm Injection

Human semen always contains a relatively high percentage of structurally abnormal spermatozoa. (1) Ordinarily, immature sperm do not complete plasma membrane remodeling to form zona pellucida binding sites, and are therefore outside of the potential fertilization pool. However, assisted reproduction techniques, most notably intracytoplasmic sperm injection (ICSI), may bypass this natural selection process and introduce the possibility of ovum fertilization by immature spermatozoa. ICSI is a particular type of *in vitro* fertilization (IVF) that requires only one sperm for successful fertilization and obviates the need for sperm to independently penetrate the zona pellucida. It is recommended for couples with severe male-factor infertility, including oligospermia ($< 20 \times 10^6$ sperm/mL), asthenospermia ($< 50\%$ of sperm having forward motion or $< 25\%$ with rapid linear motion), teratospermia ($< 30\%$ morphologically normal forms), oligoasthenoteratozoospermia (combination of all three of the aforementioned characteristics), acrosomal dysfunction, and obstructive azoospermia (absence of sperm in the ejaculate due to obstruction between the testes and the urethral meatus). ICSI begins with oocyte retrieval, as in conventional IVF procedures. Using microscopic visualization, a single motile, morphologically normal sperm is aspirated into a micropipette and microinjected beneath the zona pellucida of the harvested oocyte, directly into its ooplasm. If normal fertilization occurs, embryo transfer is performed as in conventional IVF.

Current use of ICSI for male factor infertility has met with great success.

Preliminary results concerning ICSI pregnancies have not revealed a higher incidence of

spontaneous abortion than after routine IVF. (2) Additionally, the rate of major malformations leading to functional impairment or necessitating surgery after birth is comparable to that seen in both IVF and natural conception. (3) Numerous studies, however, have found a significantly increased incidence of sex chromosomal aberrations in children born after ICSI. (2,3,4,5) Some studies have found that sex chromosome abnormalities are increased as much as four- to five-fold in ICSI offspring. (4) Sperm from infertile men requiring ICSI have shown a higher incidence of sex chromosomal aneuploidy due to nondisjunction than do sperm from fertile men. (5) The use of ICSI, therefore, clearly raises the need for genetic screening of individual spermatozoa.

Sperm Maturation

Sperm development, called spermatogenesis, consists of three main processes: mitosis, meiosis, and spermiogenesis. (Figure 1.) Diploid spermatogonia undergo mitotic proliferation to maintain a continuous supply of germ cells. Some of these spermatogonia undergo DNA replication, at which point they are labeled primary spermatocytes. These cells complete meiosis to become haploid spermatids. During spermiogenesis (also called sperm differentiation), extensive remodeling of spermatids, including development of the acrosome, tail growth, and cytoplasmic extrusion, results in highly specialized, mobile spermatozoa.

The extrusion of cytoplasm is an important step in acquiring the appropriate shape of mature sperm. Due to cytoplasmic retention, immature sperm frequently have abnormal morphology, such as asymmetrical or round heads. Because normal sperm differentiation begins only after meiotic division is completed, it is tempting to speculate

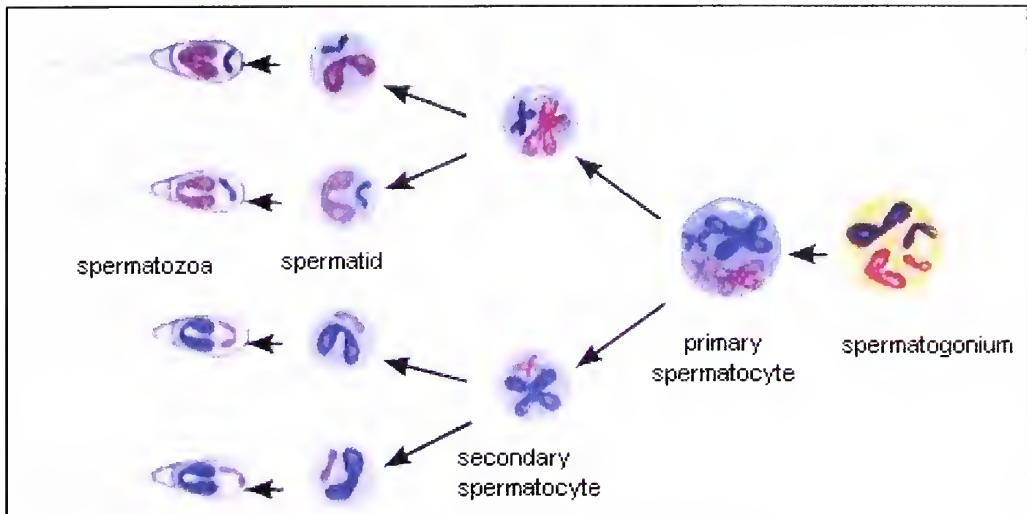


Figure 1: Phases of spermatogenesis. (6)

that a disruption of the mechanisms controlling the early stages of meiosis may be associated with inappropriate sperm development, with the subsequent production of more aneuploid and morphologically abnormal spermatozoa. (7)

Sperm Morphology

The evaluation of sperm morphology has been a difficult and inconsistent science which must take into account a great deal of natural variation. Examination of sperm recovered from postcoital cervical mucus or from the surface of zona pellucidae has helped to define the appearance of a normal spermatozoon. Complete assessment of sperm shape includes analysis of the head, neck, midpiece, and tail. In general, clinical laboratories use sperm morphology parameters proposed by the World Health Organization (WHO), the so-called “strict morphology,” developed by Kruger, which is based on shape properties of sperm bound to the zona pellucida in IVF. (8) For a spermatozoon to be considered normal, the head should be oval and symmetrical, with the ratio of the longitudinal and transverse diameters approximately 2:1. Insertion of the

tail should be axial (in line with the long axis of the head). Abnormal morphologic variants include heads that are large, small, round, or amorphous; midpieces that bulge or taper; or sperm with multiple heads or tails. The Huszar laboratory at Yale University has developed objective computer-assisted morphometry for the assessment of sperm shape and has utilized biochemical markers to more accurately assess the relationship between sperm shape, sperm maturity, and function. (9)

Biochemical Markers of Sperm Maturity

Germ cells are believed to contain the genetic programming necessary to guide their complex differentiation and development. Through developmental regulation of gene expression, the synthesis of specific proteins coincides with distinct phases of gametogenesis, and may likely guide the transition between phases. An evaluation of the cyclical expression of proteins in sperm maturation may, therefore, lead to biochemical markers of sperm maturity.

One potential biochemical marker of sperm maturity is the concentration of creatine phosphokinase (CK) in sperm. (10) CK-B, a cytoplasmic enzyme, is a marker of cytoplasmic extrusion during spermiogenesis. High levels of CK-B in sperm indicate cytoplasmic retention and have been associated with decreased fertility. (4) CK immunochemistry studies of individual spermatozoa have also demonstrated a relationship between cytoplasmic retention and abnormal sperm morphology, including larger head size, round heads, and amorphous heads. (11) Furthermore, it has been shown in CK-immunostained sperm-hemizona complexes that sperm which bind to the

zona are exclusively those of the normal mature type, without CK-B or cytoplasmic retention. (12)

A related biochemical marker of sperm maturation is the testis-specific chaperone protein HspA2, a member of the highly conserved Hsp70 chaperone family which has been thoroughly investigated in the mouse. (13) The Huszar laboratory has identified two waves of expression of HspA2 in human sperm development: in spermatocytes undergoing meiosis, and in spermatids undergoing spermiogenic maturation. (14) HspA2 first appears in primary and secondary spermatocytes likely as a component of the synaptonemal complex, the structure formed between homologous chromosomes during their synapsis in meiosis. The second wave of expression occurs during terminal spermiogenesis, along with cytoplasmic extrusion, plasma membrane remodeling, and formation of zona-binding sites. The Huszar laboratory has suggested that the underlying factor in both sperm immaturity and chromosomal aneuploidies is diminished HspA2 expression, which may cause both the higher incidence of disomies due to meiotic nondisjunction and the abnormal shape of immature sperm due to cytoplasmic retention. It has been shown that sperm morphology and the expression of HspA2 (as well as other biochemical markers) are related, because both reflect the state of spermiogenic maturity. (4)

HspA2 and Morphology

Gergely et. al. established the relationship between sperm morphology and HspA2 as a biochemical marker of sperm maturity. (9) Three sperm fractions were separated by sequential centrifugation based on the observation that immature spermatozoa with

cytoplasmic retention have lower density than normal sperm. The HspA2 ratios $[\%HspA2/(HspA2 + CK-B)]$, differed significantly between the A, B, and C fractions: HspA2 ratios were uniformly highest in the first, most dense fraction, which contains the least cytoplasm, and lowest in the third fraction. Decreased HspA2 ratios in immature spermatozoa are associated with cytoplasmic retention.

Role of HspA2 in Meiosis

In addition to its expression in spermatids and mature sperm, HspA2 is found in spermatocytes at low levels, where it is believed to chaperone meiosis. (14) In mice, a cascade of interactions, including those between Hsp70-2 and downstream cyclins and kinases, is responsible for the G2-to-M transition of meiosis II. (13)

A second potential role for HspA2 in meiosis is in directly chaperoning the disjunction of homologous chromosomes. Although the presence of HspA2 has not yet been demonstrated in human sperm synaptonemal complexes, Hsp70-2 has been found in rodent models. In mice lacking Hsp70-2, synaptonemal complexes fragment early in meiosis and paired chromosomes fail to desynapse. (13) Hsp70-2 expression abnormalities are therefore thought to be related to aneuploidies through their role in nondisjunction.

Bridging Morphology and Numerical Chromosomal Abnormalities

Numerical chromosomal abnormalities in sperm consist of aneuploidies or diploidies. In aneuploidy, a sperm cell possesses more or less than one copy of an autosomal or sex chromosome; in diploidy, a sperm possesses two copies of the entire

genome. It is difficult to estimate the true frequency of paternally-derived autosomal aneuploidies because most trisomies are eliminated early in embryogenesis. (7)

Several studies have demonstrated an association between sperm shape properties and numerical chromosomal abnormalities. Compared to the general male population, men with oligoasthenoteratozoospermia have a higher incidence of numerical chromosomal abnormalities (2.7% vs. 1.8%), suggesting that these patients produce higher proportions of aneuploid gametes. (15) Aneuploidy frequency in infertile males has been directly correlated with severity of oligospermia (2) and indirectly correlated with sperm motility. (7) Furthermore, infertile men with normal karyotypes and low sperm concentrations or higher levels of morphologically abnormal sperm have significantly increased risks of producing aneuploid spermatozoa, particularly for the sex chromosomes. (14)

A thorough review of the literature, however, reveals an inconsistent association between sperm morphology and numerical chromosomal abnormalities. Although Lee et al. (1) found that the incidence of structural chromosomal aberrations were approximately four-fold higher in semen samples with high frequencies of sperm having amorphous, round, or elongated heads as compared to those with more morphologically normal sperm, no significant difference was noted in the incidence of aneuploidies. Additionally, a case study of men with increased levels of globozoospermia (sperm that lack acrosomes), shortened flagella syndrome, or sperm with abnormal acrosomes, no association was found between sperm shape and chromosomal status. (19) Furthermore, Ryu et al. (20) studied approximately 100 - 150 morphologically normal sperm (according to the strict criteria of Kruger [8]) from both normal and infertile couples and

found that normal morphology is not an absolute indicator for the selection of genetically normal sperm.

Since a common factor between sperm immaturity and aneuploidies is HspA2 expression, it has been proposed by the Huszar laboratory that diminished expression of HspA2 leads to defects both in meiotic events and in cytoplasmic extrusion. It is thus anticipated that immature sperm which show cytoplasmic retention will also have higher incidence of disomies and aneuploidies due to meiotic impairments. (4) Although significant correlations ($r = 0.7 - 0.78$) have been found between proportions of immature sperm with cytoplasmic retention and total disomies within a sample (4), literature examining a direct association between numerical chromosomal abnormalities and individual sperm morphology is extremely limited and controversial. Abnormal sperm with large heads, micro-heads, two heads, two midpieces, or two tails have been examined and found to have nearly a 30-fold increase in aneuploidy rate over normal spermatozoa, independent of male fertility status. (7) Particularly high frequencies of aneuploidy and diploidy were found in spermatozoa with enlarged heads (40%). (7) Other studies have reported an increase in the incidence of structural chromosome abnormalities in sperm with amorphous, round, and elongated heads (26.1%) as compared to normal sperm (6.9%), but no significant difference in aneuploidy frequency. (1)

In order to better assess the relationship between sperm shape and chromosomal aberrations, it is necessary to study the same spermatozoon for both parameters. The most straightforward technique for visualizing chromosomal aneuploidies is fluorescent *in situ* hybridization (FISH). Preliminary studies of this association using *in-situ*

hybridization have been hindered by methodological factors inherent in the hybridization procedure, namely the requirement for DNA decondensation and denaturation, which increase cell size and have an unknown effect on cell shape. However, if cell shape were known to remain unchanged by the decondensation process, the association between individual sperm shape and aneuploidy could be easily examined using the FISH method. This question was studied in the Huszar laboratory, and I became part of this effort in fulfilling the Yale School of Medicine thesis requirement.

Fluorescent In Situ Hybridization

The principle behind FISH is that probes of single stranded DNA can be synthesized to incorporate fluorescent molecules (or antigenic sites that are recognized by fluorescent antibodies), and be hybridized to target DNA for direct visualization and mapping of all locations bearing the specified sequence. In order for hybridization to occur, however, DNA must first be decondensed and denatured. Sperm DNA is packed even more tightly than that in somatic cells because nuclear histones are replaced by sperm-specific protamines during spermatogenesis. Tightly coiled loops of sperm DNA are held in place by disulfide bonds formed when sulfhydryl groups on the protamines are oxidized. DNA decondensation can be achieved by the addition of dithiothreitol (DTT), which reduces the protamine disulfide bonds, unfolding the loops of DNA.

Ideally, when performing ICSI, the direct injection of chromosomally abnormal sperm into human oocytes would be avoided, minimizing the risk of aberrant fertilization.

(1) In order to do this, a method of normal haploid sperm selection that is fast, inexpensive, and accurate is required. FISH is an easy and reliable method to assess

ploidy, but it is both costly and time consuming, and, more importantly, sperm which have undergone FISH cannot be subsequently used for ICSI. Because ICSI routinely uses microscopic visualization for sperm selection, selection based on normal morphology is tempting, but an association between aneuploidies and aberrant sperm shape has never been explored at the level of the individual sperm.

Study Aims

The purpose of our work is ultimately to examine a potential relationship between sperm morphology and aneuploidy. We plan to do this by performing FISH on spermatozoa and determining whether the sperm which show aneuploidies are also those with abnormal morphology. As a subset of our work, the present study seeks to examine whether sperm with normal and abnormal morphology will maintain their original shape after DNA decondensation and denaturation. We approached this question using objective, computer-assisted morphometry of individual spermatozoa in the native shape and after decondensation and denaturation, with consideration of sperm in various morphological categories. The result of this study, namely that after decondensation and denaturation the original sperm shape is preserved, will enable us to thoroughly elucidate the relationship between sperm morphology and aneuploidy using FISH.

METHODS

Study Population

The study population consisted of men who presented for semen analysis at the Sperm Physiology Laboratory of the Department of Obstetrics and Gynecology at the Yale University School of Medicine. Samples with low sperm concentrations were selected because earlier work has demonstrated that these ejaculates are more likely to contain a high proportion of immature sperm with cytoplasmic retention, abnormal morphology, and chromosomal aneuploidies. (4, 21) In all, 21 slides from eight different patients were examined in this study. All studies were approved by the Human Investigation Committee of the Yale University School of Medicine.

Preparation of Slides

Aliquots of liquefied semen (100 - 200 μ L) from eight patients (mean concentration 16.9 ± 3.1 million sperm/mL; mean motility 43.2 ± 2.7 %) were diluted with serum physiologic saline containing 0.3% BSA and 30 mM imidazole (SAIM) to a final volume of 5 – 8 mL. Semen samples were centrifuged at 400 x g for 18 minutes at 24° C. Supernatant was discarded and pelleted sperm were resuspended in the saline-imidazole solution to a concentration of 10-25 million sperm/mL. Sperm slides were prepared by smearing 10 μ L of sample onto clean glass slides and allowing them to air-dry. Slides were subsequently fixed in a 3:1 methanol-acetic acid (MAA) solution for 15 minutes and then air-dried for 20 minutes at room temperature. Slides were dehydrated in 70%, 85%, and 100% ethanol for five minutes each, and then air-dried for 20 minutes at room temperature.

Imaging of Sperm

The basic experimental design, including preparation of slides, pre- and post-decondensation imaging of sperm, and morphometric analysis, is summarized in Figure 2.

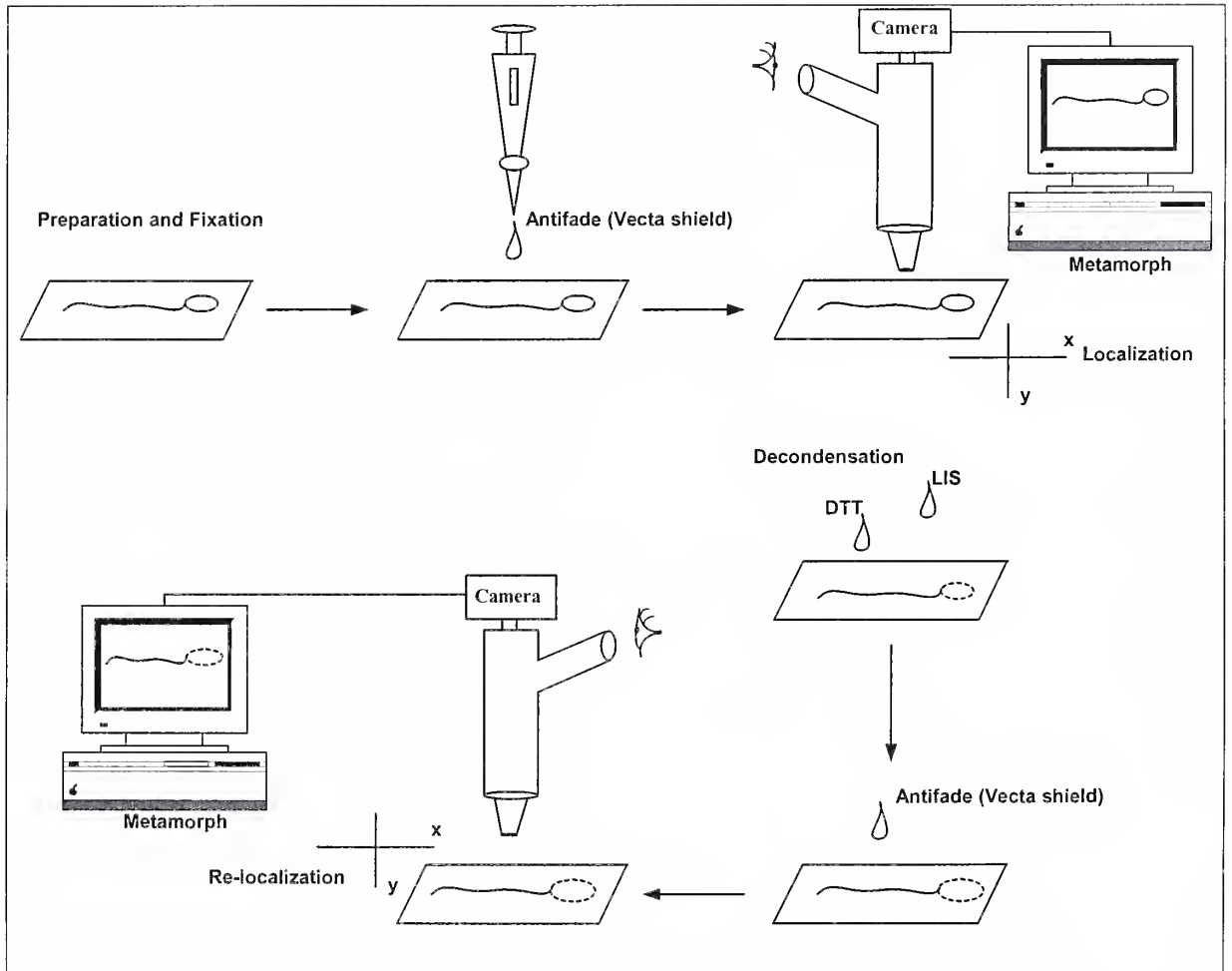


Figure 2: Experimental design.

Fixed slides were stained with one drop of antifade mounting medium (Vectashield™; Vector Laboratories, Burlingame, CA), and images were captured via a black-and-white digital camera using the 40x phase-contrast objective of an Olympus BX51 microscope (Olympus, Melville NJ). Although antifade mounting medium is not a

dye, its use proved superior to Coomassie Blue (which had previously been used) for producing images with consistently dark sperm heads and tails. Such contrast is necessary to establish a threshold level for the separation of sperm from background for the *Metamorph* assessments.

Phase-contrast images of sperm fields were digitized using a Sanyo VCB-3524 B/W CCD camera (Sanyo, Richmond, IN) and the computer program *Metamorph* (Version 4.6r1, Universal Imaging Corporation, Downingtown, PA) and were saved. The X, Y coordinates of each field digitized were noted on the microscope stage. In addition, the characteristic configuration of sperm cells in each field was sketched in a notebook in order to aid in relocation of the sperm field.

After the decondensation step, the same fields as had been studied initially were recaptured, and the now-decondensed sperm fields were digitized and saved for subsequent analysis using *Metamorph*.

Decondensation

Slide cover slips that were placed for initial microscopic observation were carefully removed by rinsing with distilled water. Slides were placed in a humidity chamber and decondensed by flooding with 1250 μ L of a 10 mM solution of dithiothreitol (DTT) (Sigma, St. Louis, MO) in 0.1 M Tris-HCl (pH 8.0) (American Bioanalytical, Natick, MA) for 20 minutes at room temperature. The DTT solution was discarded, and slides were returned to the humidity chamber and flooded with 1000 μ l of a 10mM solution of LIS (lithium 3,5-diiodosalicylic acid) (Sigma) in 0.1 M Tris-HCl (pH 8.0). Slides were incubated in the dark for 2.5 hours at room temperature. The LIS

solution was discarded and slides were rinsed gently in distilled water. Slides were stained, as initially, with one drop of Vectashield antifade mounting medium before new cover slides were placed on them.

Calibration

Calibration was performed by viewing an objective micrometer scale (OB-M 1/100) at 40x magnification and digitizing the image with the *Metamorph* program. Using the *Metamorph* drawing feature, a line was drawn on the micrometer image, and its length was set to 10 μm . The automated, computerized conversion of pixels to μm set our calibration at 0.29 $\mu\text{m}/\text{pixel}$.

Computerized Morphometry Measurements

After digitizing the images, *Metamorph* overlay tools were used to delineate the head versus tail regions of individual spermatozoa. Images were viewed using an inclusive threshold for dark objects in order to identify regions for measurement.

Metamorph was used to measure sperm head parameters with selected morphometry standards inherently defined by the program. (Figure 3.) The relevance of each to sperm head morphology is straightforward: area (area of entire object), perimeter (distance around edge of object, measuring from midpoints of each pixel that defines its border), long axis of the head (length of longest chord through the object), short axis of the head (width measured perpendicular to the longest chord), and shape factor ($4\pi A/P^2$, a value between 0-1 representing how closely object approximates a circle, with 1 being a perfect circle). The sperm tail length was measured as fiber length (length of an object,

assuming that it is fiber-like in nature). In addition, we developed two sperm head parameters that are not standard to the *Metamorph* program which reflect sperm cellular maturity: roundness ratio (short axis of the head: long axis of the head), and the ratio of tail length to the long axis of the head. These parameters were calculated using Microsoft Excel (Microsoft, Redmond, WA).

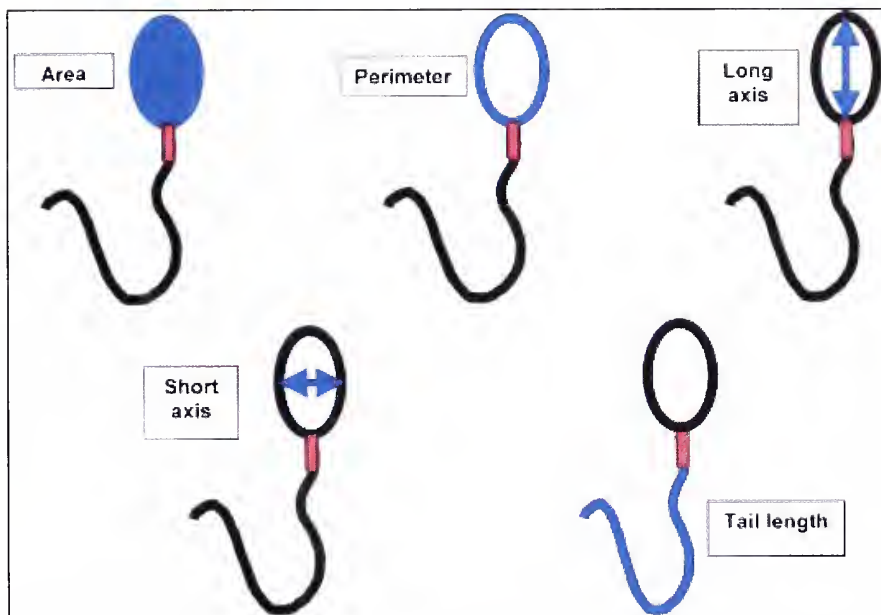


Figure 3: *Metamorph*-generated sperm head and tail parameters.

Morphological Classification by Sperm Head

Sperm cells were classified into four groups by visual inspection (Figure 4): symmetrical ($n = 115$), or sperm that were normally shaped with oval, symmetrical heads and axial tail insertion; irregular ($n = 115$), or sperm with large, round, or asymmetrical heads, bulging midpieces, and/or abaxial tail insertions; asymmetrical ($n = 115$), or sperm that did not satisfy the descriptions of symmetrical or irregular sperm because of tapered

and/or elongated or slightly rounded heads, moderately enlarged midpieces, slightly asymmetrical postacrosomal regions, etc.; or amorphous (n = 50), or sperm with grossly

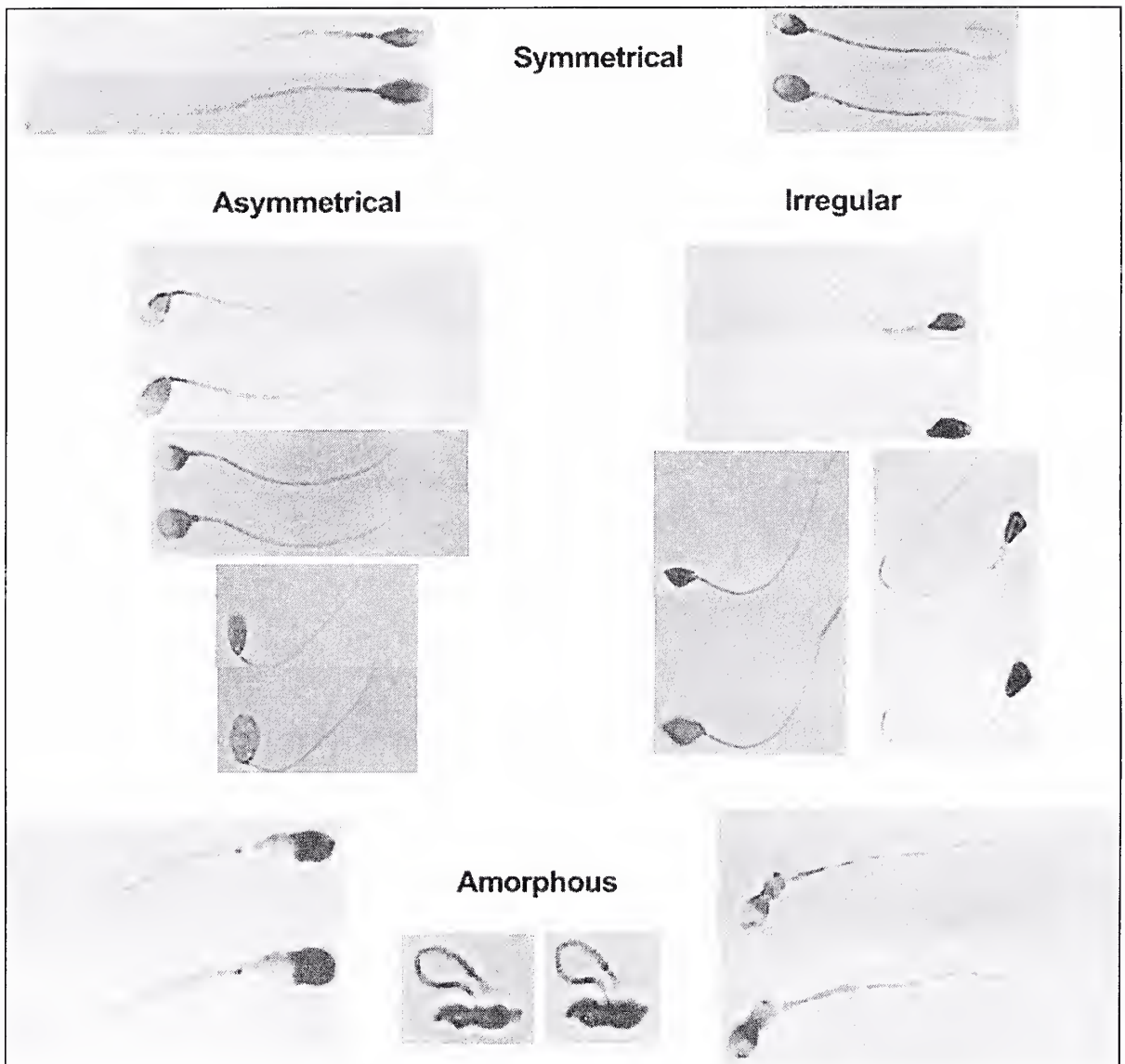


Figure 4: Pre- and post-decondensation images of sperm in the various shape categories. Sperm were classified according to their head shape as symmetrical, asymmetrical, irregular, or amorphous. Observe the maintenance of shape in the decondensed state. Magnification \sim x1500.

asymmetric and distorted heads. This classification distinguishes among the various morphologic types of mature and immature spermatozoa; it has no relationship to the

andrological or clinical assessments of normal or abnormal sperm morphology.

Classification was performed visually in order to more accurately simulate the selection of sperm for ICSI, in which samples cannot be fixed and, therefore, cannot be evaluated using *Metamorph*.

Statistical Analysis

Sperm shape parameters before and after decondensation were compared using the paired student t-test with *SigmaStat* (Version 2.0, Jandel Scientific Corporation, San Rafael, CA) within each shape category. Percent change in the mean for each parameter after decondensation was also calculated. Differences before and after decondensation within each of the different sperm shape categories (symmetrical, asymmetrical, irregular, and amorphous) were analyzed using one-way ANOVA and post hoc Dunn tests with a $p < 0.05$ level of significance.

We determined the interrater reliability of *Metamorph* assessments by measuring the various parameters five different times in the same sperm ($n = 70$ sperm; 3500 measurements in all). The measurements were performed by two different investigators working independently (Catalanotti and Celik-Ozenci).

Denaturation

Because the FISH protocol calls for decondensation followed by denaturation to make DNA fully accessible to probes, we tested the effect of denaturation on the size and shape of decondensed sperm. One hundred sperm from each of three men ($n = 300$) were studied. Decondensed sperm (as described above) were subsequently treated with

denaturation solution (28 mL of 70% formamide and 4 mL of 20 x SSC [1 x SSC: 0.15 M sodium chloride and 0.015 M sodium citrate]) and then heated to 75° C for ten minutes. The denatured slides were immediately cooled to -20° C in 70% ethyl alcohol for two minutes and then in 100% ethyl alcohol for two minutes. Slides were allowed to air-dry and were stained with one drop of Vectashield antifade mounting medium for imaging.

Validation of Methods

To ensure that antifade mounting medium for fluorescence has no effect on sperm size and shape and to be sure that its use does not block DNA decondensation with DTT, the above experiment was performed substituting one drop of distilled water for mounting medium (n = 30). All *Metamorph* measurements were compared to a trial using the same sperm subsequently mounted with Vectashield antifade mounting medium (20 sperm each from the symmetrical, asymmetrical, and irregular groups, and 10 amorphous sperm; n = 70) using the paired student t-test.

To demonstrate that changes in sperm size are directly related to the DTT-induced decondensation and not to the swelling effect of LIS, three slides from each semen sample were incubated with DTT alone, with LIS alone, with LIS followed by DTT, or with DTT followed by LIS. The sperm head dimensions were determined before and after treatment.

To ensure that the majority of sperm undergo decondensation in response to DTT-LIS treatment and that sperm selected for measurements are typical in this regard, we reviewed 100 sperm from each of the eight men (800 sperm in all). We determined the percentage that appeared to be decondensed, over-decondensed, and not decondensed.

Sperm that were not decondensed or that were over-decondensed were not further evaluated in this study.

FISH Study

Preliminary FISH studies relating sperm morphology and aneuploidy were performed by Celik-Ozenci (22) using the method described by Kovanci, et al. (23). Thirty slides with sperm from 15 men were fixed and decondensed using DTT and LIS solutions, as described above. Overall, 1286 spermatozoa were visualized and evaluated for both morphology and aneuploidy. Three probes were used for FISH (Vysis, Downers Grove, IL): (1) X chromosome: Xp11-Xp21 labeled with biotin-16-dUTP by nick translation; (2) Y chromosome: Vysis alpha satellite rhodamine-labelled probe; (3) chromosome 17: alpha satellite sequence-specific probe labeled with both biotin-16-dUTP and digoxigenin-11-dUTP by nick translation. A 12 μ L sample of hybridization mixture (50% formamide and 10% dextran sulfate in 2xSSC) containing the probes was denatured at 75 – 80° C for eight minutes and applied to the slides. The X, Y, and 17 probes were simultaneously hybridized to the slides in a moist chamber for 12-14 hours. Sperm slides were incubated with avidin-FITC (fluorescence green) for biotin-labeled probes, and anti-digoxigenin-rhodamine (fluorescence red) for digoxigenin-labeled probes. The use of both biotin and digoxigenin labels on the probe for chromosome 17 resulted in a yellow color (the combination of red and green fluorescence gives yellow). Slides were stained with 4',6-diamidino-2-phenylindole, mounted with antifade, and viewed for fluorescence. Sperm were considered disomic when they showed two fluorescent domains of same color, comparable in size and brightness, in approximately

the same focal plane, clearly positioned inside the edge of the sperm head and at least one domain apart. Diploidy was recognized by the presence of two double fluorescence domains with the above criteria.

Slides were also viewed with a 40x phase-contrast objective in order to assess morphology and to exclude apparent diploidy in two spermatozoa in close proximity to each other. The 1286 spermatozoa were classified as symmetrical, asymmetrical, irregular, or amorphous by visual inspection, and the distribution of haploid, disomic, and diploid sperm within each category was determined. In addition, two investigators independently assessed the sperm for Kruger strict morphology scores (8). Data were statistically analyzed using one-way ANOVA rank tests and post hoc Dunn tests.

RESULTS

Decondensation and Relocalization of Sperm Fields

Overall, our decondensation protocol was effective, as $82.2\% \pm 2.2\%$ of sperm were decondensed, $12.2\% \pm 2.0\%$ were over-decondensed, and $5.0\% \pm 1.2\%$ were not decondensed ($n = 800$) (data not shown). Sperm that were over-decondensed or not decondensed were not evaluated in this study. In evaluating the effects of decondensation on sperm shape in the eight men studied, we digitized 307 fields of the native, pre-decondensed sperm representing all four shape categories of spermatozoa. Of these 307 fields, we were able to relocalize 277 fields (90%) after the decondensation step, with 395 sperm available for analysis in all. (Figure 5.)

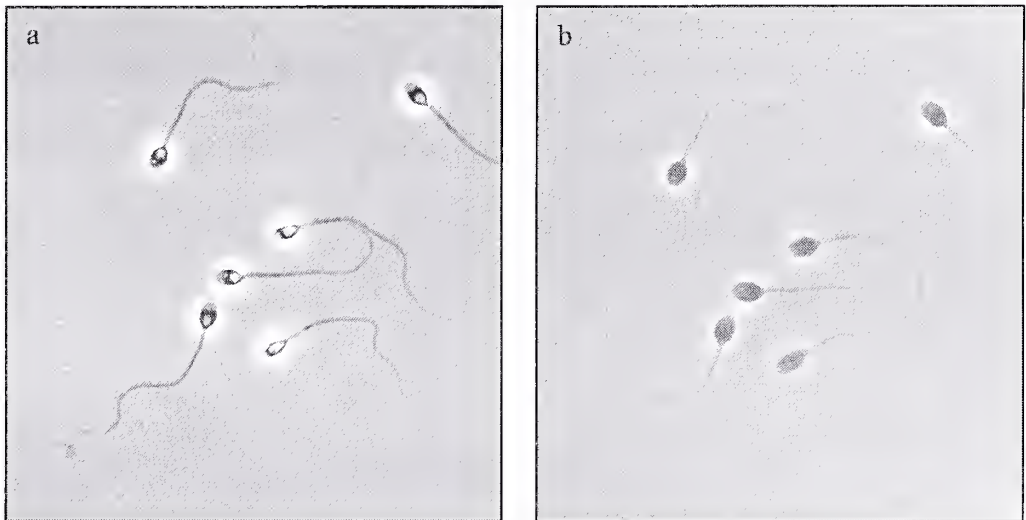


Figure 5: Sperm field before (a) and after (b) decondensation. Note the characteristic configuration of fixed sperm, aiding in the relocalization of sperm fields. Also note the visual preservation of sperm head shape. Magnification $\sim x 1500$.

We performed morphological classification of the sperm heads by conventional microscopic assessment. Because the irregular and amorphous types were more common

in certain samples, while samples from any man have many symmetrical and asymmetrical sperm, we captured more fields in samples from some men than from others.

Controls

Antifade application does not affect sperm size or shape, as no significant differences were seen between individual sperm dyed with water and with antifade in any parameters measured ($n = 30$)(data not shown). Interobserver agreement was found in $96.6\% \pm 0.6\%$ (data not shown) of measurements. The highest variation between observers was seen in the assessment of head area (5.9%) and the lowest variation in the assessment of short axis (2.4%), whereas the perimeter, long axis, and tail length measurements all showed a 2.9% variation.

Sperm treated with DTT showed less than 10% increases ($p < 0.05$, data not shown) in each head parameter, with no significant changes in shape factor. Sperm treated with LIS alone showed less than 20% increases in head parameters and head area ($p < 0.001$ and $p = 0.005$, respectively). The combined effects of DTT and LIS, when LIS is applied first, resulted in a change in head size of only 25%. However, sperm treated with DTT and then LIS, as in the present protocol, showed increases comparable to those indicated by our data (area: + 40%; perimeter: + 22%, long axis: + 22%, short axis: +15%; all $p < 0.001$, with no significant changes in shape factor; $n = 250$). No significant differences were noted after denaturation in any parameters measured by *Metamorph* ($n = 300$) (data not shown).

Decondensation Increases Sperm Size

Significant differences were seen in the comparisons of sperm dimensions in the native and decondensed states across all groups. All head parameters increased significantly as a result of decondensation ($p < 0.001$ for all). Mean values for the initial and post-decondensation parameters within each morphological category are shown in Table 1. Decondensation-related changes were consistent across shape categories, as similar increases in all head parameters were observed within a narrow range. (Table 2.) For example, the four values were very close in change in perimeter (mean and range: 23.5% and $5\mu\text{m}$, respectively), in long axis (18.5% and $6\mu\text{m}$, respectively), and in short axis (21.8% and $2\mu\text{m}$, respectively). The area parameter did not quite follow this pattern because the amorphous sperm group showed a higher percentage change. However, the areas of the symmetrical, asymmetrical, and irregular groups were similar (52.3% and $7\mu\text{m}$, respectively). Because the tail is a one-dimensional object lacking its own DNA, its length was not affected by the decondensation, and it is not considered in the tables.

Conservation of Sperm Shape after Decondensation

Initial shape was preserved across all morphological categories as measured either by roundness ratio, by shape factor, or by both. (Table 3.) Symmetrical sperm showed a 0% change in roundness ratio ($p > 0.05$) and a 4% change in shape factor ($p < 0.001$). Asymmetrical sperm showed a 4% change in roundness ratio ($p < 0.001$) and a 0% change in shape factor ($p > 0.05$). Irregular sperm showed a 3% change in roundness ratio ($p < 0.001$) and a 1.2% change in shape factor ($p > 0.05$). Amorphous sperm showed a 0% change in roundness ratio ($p > 0.05$) and a 1.3% change in shape factor (p

> 0.05). Thus, significant changes included only very small increases in roundness ratio among asymmetrical and irregular sperm and in shape factor among symmetrical sperm, with no change greater than 4%.

FISH Observations

Of the spermatozoa studied, 367 were symmetrical, 368 were asymmetrical, 504 were irregular, and 47 were amorphous (n = 1286). As Figure 6 indicates, relationships between numerical chromosomal aberrations and sperm shapes were inconsistent. Haploid and aberrant nuclei were seen in the heads of sperm with both normal and abnormal shapes. Disomic and diploid sperm were present in all morphological categories, with their frequency increasing along with increased shape abnormality. (Table 4.) There was a significantly higher frequency of aneuploidies in the irregular and amorphous shape groups as compared to the symmetrical and asymmetrical categories ($p < 0.001$). However, even "normal" appearing symmetrical spermatozoa included 68 sperm (of the 386 total aneuploid sperm) with numerical chromosomal abnormalities. The Kruger strict morphology scores of the haploid (n = 900), disomic (n = 256), and diploid (n = 13) sperm were 24%, 10%, and 1%, respectively.

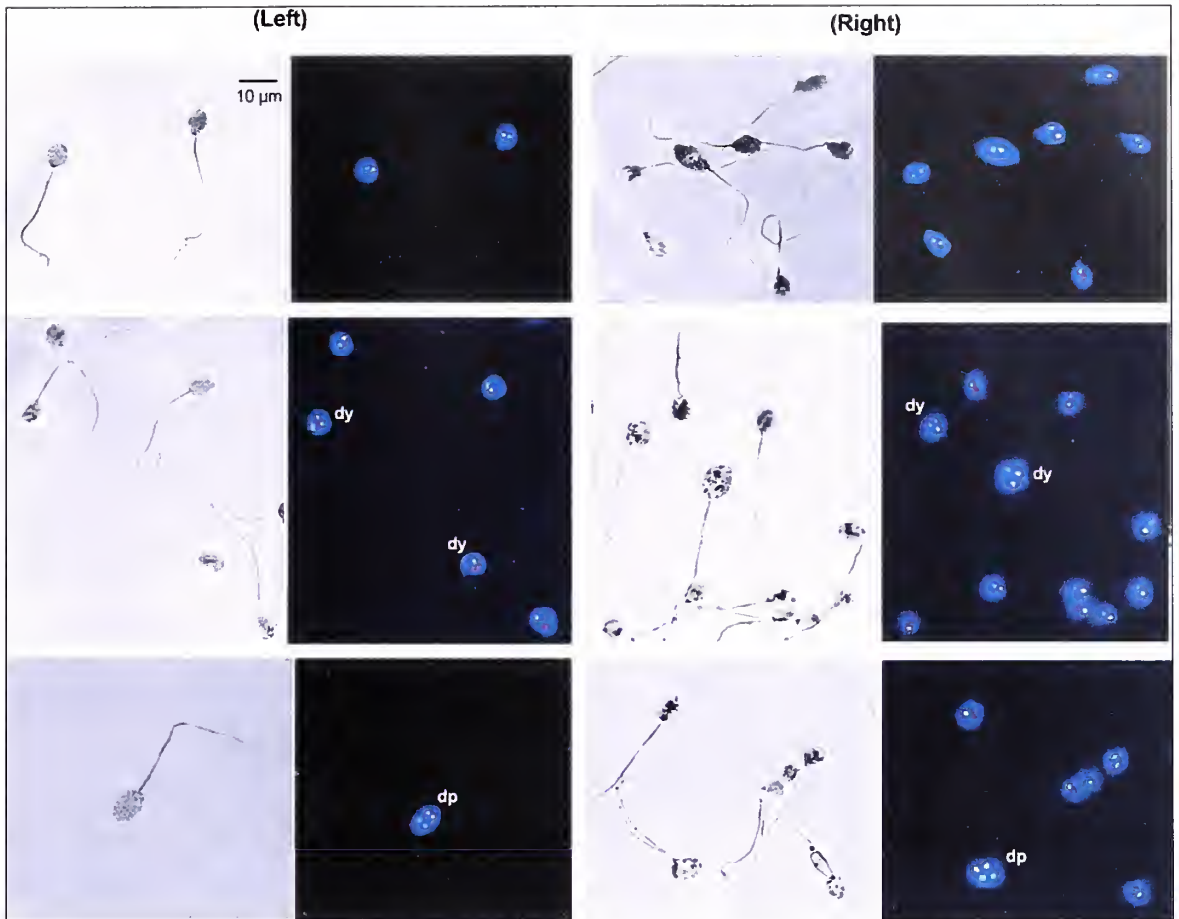


Figure 6: Shape and chromosomal properties of decondensed sperm with phase-contrast microscopy and FISH. *Left:* Sperm with normal morphology; *Right:* Sperm with abnormal morphology. *Top:* Sperm with haploid nuclei; *Middle:* Sperm with disomic nuclei (dy); *Bottom:* sperm with diploid nuclei (dp). Magnification x600.

	Initial				Decondensed			
	Symmetrical (n = 115)	Asymmetrical (n = 115)	Irregular (n = 115)	Amorphous (n = 50)	Symmetrical (n = 115)	Asymmetrical (n = 115)	Irregular (n = 115)	Amorphous (n = 50)
Area (μm^2)	14.3 \pm 0.2	15.4 \pm 0.3	21.2 \pm 0.6	24.7 \pm 1.5	21.7 \pm 0.6	22.9 \pm 0.7	33.1 \pm 1.1	46.0 \pm 5.3
Perimeter (μm)	15.0 \pm 0.1	16.4 \pm 0.2	19.4 \pm 0.3	21.2 \pm 0.8	18.7 \pm 0.3	19.7 \pm 0.3	24.1 \pm 0.4	26.4 \pm 1.1
Long axis (μm)	5.8 \pm 0.1	6.6 \pm 0.1	7.5 \pm 0.2	7.6 \pm 0.3	7.0 \pm 0.1	7.6 \pm 0.1	8.8 \pm 0.2	9.2 \pm 0.4
Short axis (μm)	4.7 \pm 0.03	4.6 \pm 0.1	5.6 \pm 0.1	6.0 \pm 0.2	5.7 \pm 0.01	5.6 \pm 0.1	6.9 \pm 0.1	7.4 \pm 0.3
Shape factor	0.89 \pm 0.01	0.80 \pm 0.01	0.79 \pm 0.01	0.76 \pm 0.02	0.85 \pm 0.01	0.80 \pm 0.01	0.78 \pm 0.01	0.75 \pm 0.02
Roundness ratio	0.82 \pm 0.01	0.71 \pm 0.01	0.79 \pm 0.02	0.83 \pm 0.03	0.82 \pm 0.01	0.74 \pm 0.01	0.81 \pm 0.02	0.83 \pm 0.02
Tail : long axis	10.3 \pm 0.2	9.1 \pm 0.2	7.4 \pm 0.2	7.7 \pm 0.4	8.6 \pm 0.2	7.9 \pm 0.2	6.5 \pm 0.2	6.8 \pm 0.3

Table 1: Pre- and post-decondensation measurements. Values are indicated as mean \pm SEM.

Values in red in decondensed sperm indicate changes when compared to initial sperm ($p < 0.001$).

Values in blue in decondensed sperm indicate changes which are not significant when compared to initial sperm ($p > 0.05$).

- Note that shape factor shows a small but significant change with decondensation only among symmetrical sperm.
- Roundness ratio is not significantly altered by decondensation among symmetrical or amorphous sperm.

	Symmetrical (n = 115)	Asymmetrical (n= 115)	Irregular (n = 115)	Amorphous (n = 50)
Area (μm^2)	52%	49%	56%	87%
Perimeter (μm)	25%	20%	24%	25%
Long axis (μm)	21%	15%	17%	21%
Short axis (μm)	21%	22%	23%	21%

Table 2: Percent increases in mean values for size parameters after decondensation across shape categories. All are significant changes when compared to initial size parameters ($p < 0.001$).

	Symmetrical (n = 115)	Asymmetrical (n= 115)	Irregular (n = 115)	Amorphous (n = 50)
Shape factor	4%	0%	1.2%	1.3%
Roundness ratio	0%	4%	3%	0%

Table 3: Percent changes in mean values for shape parameters after decondensation across shape categories. Values in red are significant changes when compared to initial values ($p < 0.001$).

Shape Category	No Numerical Chromosomal Abnormalities (n = 900)	Disomy (n = 256)	Diploidy (n = 130)
Symmetrical (n=367)	299	63	5
Asymmetrical (n=368)	301	59	8
Irregular (n=504)	299	119	86
Amorphous (n=47)	1*	15	31

Table 4: Number of disomic and diploid sperm within each morphological category. (n = 1286)
Values in red are significant when compared with symmetrical and asymmetrical sperm categories (p < 0.001).
* Also significant when compared with irregular sperm (p < 0.001).

DISCUSSION

Several laboratories have reported data supporting a relationship between abnormal sperm morphology and increased frequency of aneuploidies in semen samples, but not within a single sperm. It has been suggested that abnormal sperm morphology, due to arrested sperm maturation and cytoplasmic retention, and increased numerical chromosomal aberrations are related to meiotic and spermiogenetic errors associated with diminished expression of HspA2. (4, 14) To our knowledge, however, the common occurrence of these two attributes within the same sperm cell has not previously been studied. The primary reason for the lack of such data is uncertainty concerning the effects of decondensation and denaturation, which are necessary for FISH, on morphological characteristics of the spermatozoa studied.

To study the potential relationship between sperm morphology and numerical chromosomal aberrations in the same sperm, we examined whether original sperm shape is conserved after the decondensation and denaturation steps that are necessary in order to make DNA accessible for hybridization by FISH probes. Although a recent brief communication reported that FISH studies may be carried out in sperm without a decondensation step (24), the data lacked controls and examined < 1000 sperm in total, rendering it of questionable merit.

We utilized the morphometry software, *Metamorph*, for objective measurements of sperm both before and after the decondensation process. To examine potential differences in decondensation-related changes between sperm with normal and abnormal shapes, the sperm dimensions in the native and decondensed states were compared within symmetrical, asymmetrical, irregular, and amorphous sperm categories. We analyzed the

maintenance of individual sperm shape in each group after decondensation. The data have been confirmatory across all morphological categories: sperm heads become larger after decondensation, but the head shape remains conserved, as evidenced by the preservation of shape factor and roundness ratio.

Decondensation consistently increases sperm head size. For each parameter measured, including head perimeter, long axis, short axis, and area, the percent increases as a result of decondensation were quite similar across morphological categories, with the exception of a larger percent increase in the mean head area among amorphous sperm. It is unclear why amorphous sperm heads increase in area to a much greater extent as a result of decondensation, but it may relate to their immature membrane structures in light of their potential for arrested maturation. (25)

Decondensation does not change sperm shape. Most sperm studied showed no significant change in shape factor or roundness ratio as a result of decondensation, and those that did showed only very small changes ($< 4\%$). Sperm shape is preserved, as determined not only visually, but also by objective morphometry, after the decondensation and denaturation protocols. The increases in the dimensions contributing to the shape factor and roundness ratio are, therefore, proportional. Sperm that undergo FISH maintain their original shapes with high fidelity. Thus, post-FISH shape can be further used to evaluate relationships between sperm shape and numerical chromosomal abnormalities.

We have carefully validated our methods by testing the technical aspects of our protocol. We established that the mounting medium does not affect decondensation or perceived sperm size after digitization. The overall efficiency of decondensation was

high, with 82.0% of sperm being appropriately decondensed and only 5.0% and 13.0% of the sperm remaining non-decondensed and over-decondensed, respectively. The interobserver agreement of *Metamorph* measurements was greater than 96%. Finally, we also investigated the effects of denaturation on sperm morphology, noting that after the decondensation process, denaturation does not cause any further appreciable increase in sperm head dimensions, and the shape of sperm is still preserved.

Our preliminary FISH observations indicate that aneuploid nuclei may be found within abnormally or normally shaped sperm heads, but occur with higher frequency in amorphous sperm. Even the most normal appearing sperm could be disomic or diploid, although diploidy is less prevalent among sperm with normal shape. Thus, visual assessment is likely an unreliable method for ICSI selection of sperm. These data are in agreement with those published by Ryu, *et al.* wherein it was found that normal morphology is not an absolute indicator for the selection of genetically normal sperm. (20) In that study, normal sperm from teratozoospermic men showed a 1.8 – 5.5% aneuploidy rate as compared to 0 – 2.6% among normal sperm in fertile controls. Normal morphology likely does not correlate perfectly with genetic normality, but abnormal head shape due to cytoplasmic retention may be associated with an increased rate of aneuploidy, as shown in the work of Kovanci *et al.* (4)

Given the increased frequency of numerical chromosomal abnormalities among semen samples from infertile men who are ICSI candidates, counseling for infertile couples undergoing ICSI should focus on the increased risk of aneuploidies, and on the phenotypic outcomes of trisomy for different chromosomes, especially sex chromosomes.

At present, it is generally accepted that there is an increase of at least 1% in the risk of sex chromosome abnormalities for children conceived by ICSI. (3)

Counseling to couples pursuing ICSI may be particularly important in cases where morphologically abnormal or immature sperm are selected for injection, as in men with 100% abnormal sperm forms. In these men, the potential to transmit abnormal genetic traits to the next generation is a major concern. Some authors have suggested that ICSI should not be recommended to patients presenting with macrocephalic spermatozoa given their increased potential for aneuploidies as compared to sperm with other abnormalities (i.e. shortened flagellae, globozoospermia, or irregular acrosomes). (19, 26)

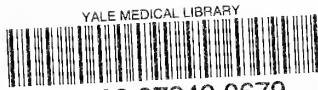
Preliminary evidence suggests that only sperm with normal morphology should be selected for ICSI, but even this precaution does not guarantee haploidy. Given the results of this study, that DNA decondensation and denaturation as required by the FISH protocol do not change sperm shape, the Huszar laboratory plans to further examine the relationship between sperm shape and numerical chromosomal abnormalities at the cellular level using visual inspection, FISH, and the *Metamorph* program. Since our preliminary work suggests an imperfect correlation, the Huszar laboratory will also evaluate sperm selection based on the presence of absence of certain plasma membrane receptors that are associated with normal sperm development. (27, 28)

REFERENCES

1. Lee JD, Kamiguchi Y, Yanagimachi R. 1996. Analysis of chromosome constitution of human spermatozoa with normal and aberrant head morphologies after injection into mouse oocytes. *Hum Reprod.* 11:1942-1946.
2. Rives N, Saint Clair A, Mazurier S, Sibert L, Siméon N, *et al.* 1999. Relationship between clinical phenotype, semen parameters and aneuploidy frequency in sperm nuclei of 50 infertile males. *Hum Genet.* 105:266-272.
3. Bonduelle M, Aytoz A, Van Assche E. 1998. Incidence of chromosomal aberrations in children born after assisted reproduction through intracytoplasmic sperm injection. *Hum Reprod.* 13:781-782.
4. Kovanci E, Kovacs T, Moretti E, Vigue L, Bray-Ward P, *et al.* 2001. FISH assessment of aneuploidy frequencies in mature and immature human spermatozoa classified by the absence or presence of cytoplasmic retention. *Hum Reprod.* 16:1209-1217.
5. Storeng RT, Plachot M, Theophile D, Mandelbaum J, *et al.* 1998. Incidence of sex chromosome abnormalities in spermatozoa from patients entering an IVF or ICSI protocol. *Acta Obstet Gynecol Scand.* Feb 77(2): 191-197 (Abstr).
6. http://www.rlc.dcccd.edu/MATHSCI/reynolds/2402lab_prac/2402pract12_sum.html (09 January 2005, 11:30am)
7. Bernardini L, Borini A, Preti S. *et al.* 1998. Study of aneuploidy in normal and abnormal germ cells from semen of fertile and infertile men. *Hum Reprod.* 13:3406-3413.
8. World Health Organization. 1999. WHO Laboratory Manual for the Examination of Human Semen and Sperm-Cervical Mucus Interaction. Fourth edition. Cambridge University Press, Cambridge, UK.
9. Gergely A, Kovanci E, Senturk L, Cosmi E, Vigue L, *et al.* 1999. Morphometric assessment of mature and diminished-maturity human spermatozoa: sperm regions that reflect differences in maturity. *Hum Reprod.* 14(8):2007-2014.
10. Huszar G, Vigue L. 1990. Spermatogenesis-Related Change in the Synthesis of the Creatine Kinase B-Type and M-Type Isoforms in Human Spermatozoa. *Mol Reprod Dev.* 25:258-262.
11. Huszar G, Vigue L. 1993. Incomplete Development of Human Spermatozoa Is Associated With Increased Creatine Phosphokinase Concentration and Abnormal Head Morphology. *Mol Reprod Dev.* 34:292-298.

12. Huszar G, Vigue L, Oehninger S. 1994. Creatine kinase (CK) immunocytochemistry of human hemizona-sperm complexes: selective binding of sperm with mature CK-staining pattern. *Fertil Steril*. 61:136-142.
13. Eddy E. 1999. Role of heat shock protein HSP70-2 in spermatogenesis. *Rev of Reprod*. 4:23-30.
14. Huszar G, Stone K, Dix D, Vigue L. 2000. Putative creatine kinase M-Isoform in human sperm is identified as the 70-kilodalton heat shock protein HspA2. *Biol Reprod*. 63:925-932.
15. Colombero LT, Hariprashad JJ, Tsai MC, Rosenwaks Z, Palermo GD. 1999. Incidence of sperm aneuploidy in relation to semen characteristics and assisted reproductive outcome. *Fertil Steril*. 72:90-96.
16. Shi Q, Martin RH. 2001. Aneuploidy in human spermatozoa: FISH analysis in men with constitutional chromosomal abnormalities, and in infertile men. *Reproduction*. 121:655-666.
17. Yakin K, Kahraman S. 2001. Certain forms of morphological anomalies of spermatozoa may reflect chromosomal aneuploidies. *Hum Reprod*. 16:1779-1780.
18. Yurov YB, Saias MJ, Vorsanova SG, Erny R, Soloviev IV, Sharonin VO, *et al*. 1996. Rapid chromosomal analysis of germ-line cells by FISH: an investigation of an infertile male with large-headed spermatozoa. *Mol Hum Reprod*. 2:665-668.
19. Viville S, Mollard R, Bach ML, Falquet C, Gerlinger P, Warter S. 2000. Do morphological anomalies reflect chromosomal aneuploidies? Case report. *Hum Reprod*. 15:2563-2566.
20. Ryu HM, Lin WW, Lamb DJ, Chuang W, Lipshultz LI, Bischoff FZ. 2001. Increased chromosome X, Y, and 18 nondisjunction in sperm from infertile patients that were identified as normal by strict morphology: implication for intracytoplasmic sperm injection. *Fertil Steril*. 76:879-83.
21. Huszar G, Corrales M, Vigue L. 1988. Correlation between sperm creatine phosphokinase activity and sperm concentrations in normospermic and oligospermic men. *Gamete Res*. 19:67-75.
22. Celik-Ozenci C, Jakab A, Kovacs T, Catalanotti J, Demir R, *et al*. 2004. Selection for ICSI: shape properties do not predict the absence or presence of numerical chromosomal aberrations. *Hum Reprod*. 19(9): 2052-2059.

23. Kovanci E, Kovacs T, Moretti E, Vigue L, Bray-Ward P, *et al.* 2001. FISH assessment of aneuploidy frequency in mature and immature human spermatozoa classified by the absence or presence of cytoplasmic retention. *Hum Reprod.* 16(6):1209-1217.
24. Almeida Santos T, Dias C, Brito R, Henriques P, Almeida Santos A. 2002. Short Communication: Analysis of Human Spermatozoa by Fluorescence In Situ Hybridization with Preservation of the Head Morphology Is Possible by Avoiding a Decondensation Treatment. *J Asst Reprod and Gen.* 19(6):291-294.
25. Huszar G, Sbracia M, Vigue L, Miller DJ, Shur BD. 1997. Sperm plasma membrane remodeling during spermiogenetic maturation in men: relationship among plasma membrane B-1,4-galactosyltransferase, cytoplasmic creatine phosphokinase, and creatine phosphokinase isoform ratios. *Biol Reprod.* 56:1020-1024.
26. Devillard F, Metzler-Guillemain C, Pelletier R, DeRobertis C, Bergues U, *et al.* 2002. Polyploidy in large-headed sperm: FISH study of three cases. *Hum Reprod.* 17(5):1292-1298.
27. Huszar G, Celik-Ozenci C, Cayli S, Zavaczki Z, Hansch E, *et al.* 2003. Hyaluronic acid binding by human sperm indicates cellular maturity, viability and unreacted acrosomal status. *Fertil Steril.* 79:1616-1624.
28. Cayli S, Jakab A, Ovari L, Delpiano E, Celik-Ozenci C, *et al.* 2003. Biochemical markers of sperm function: male fertility and sperm selection for ICSI. *Reprod Biomed Online.* 7:462-468.



**HARVEY CUSHING/JOHN HAY WHITNEY
MEDICAL LIBRARY**

MANUSCRIPT THESES

Unpublished theses submitted for the Master's and Doctor's degrees and deposited in the Medical Library are to be used only with due regard to the rights of the authors. Bibliographical references may be noted, but passages must not be copied without permission of the authors, and without proper credit being given in subsequent written or published work.

This thesis by
has been used by the following person, whose signatures attest their acceptance of the above restrictions.

NAME AND ADDRESS

DATE

